ADVANCED OPTICAL MATERIALS

# Supporting Information

for *Advanced Optical Materials,* DOI: 10.1002/adom.201701316

# Processing-Dependent Microstructure of AgCl–$CsAgCl_2$ Eutectic Photonic Crystals

*Jaewon Choi, Ashish A. Kulkarni, Erik Hanson, Daniel Bacon-Brown, Katsuyo Thornton, and Paul V. Braun**

# Supporting Information

## Processing-Dependent Microstructure of AgCl-$CsAgCl_2$ Eutectic Photonic Crystals

*Jaewon Choi[±], Ashish A. Kulkarni[±], Erik Hanson, Daniel Bacon-Brown, Katsuyo Thornton and Paul V. Braun[*]*

[±] contributed equally to this work

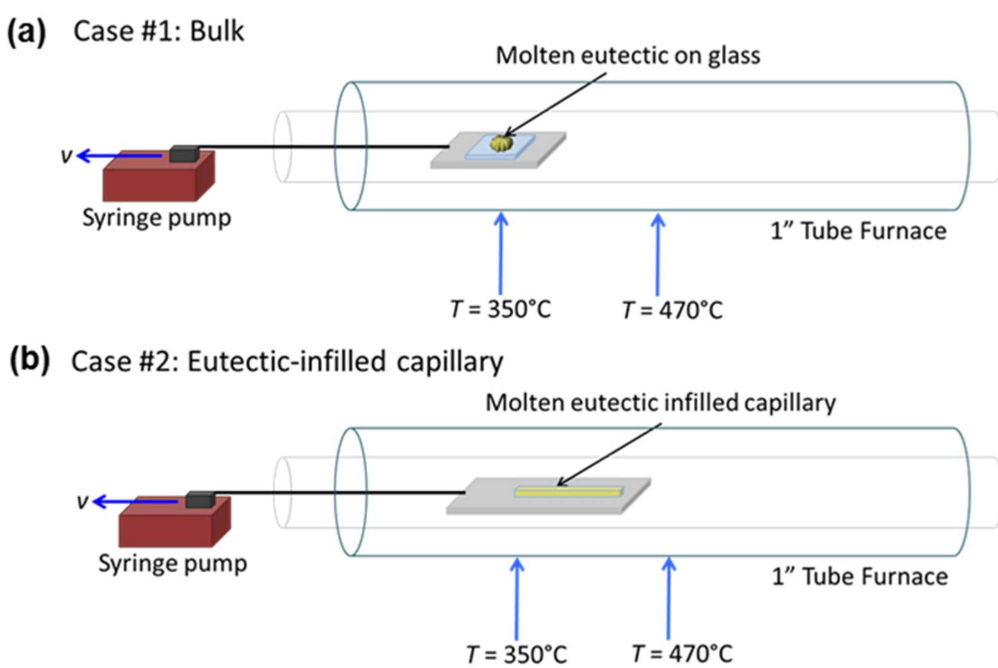

Figure S1: Schematic of the experimental setup for directional solidification of (a) bulk and (b) capillary samples. See the Experimental Section for details.

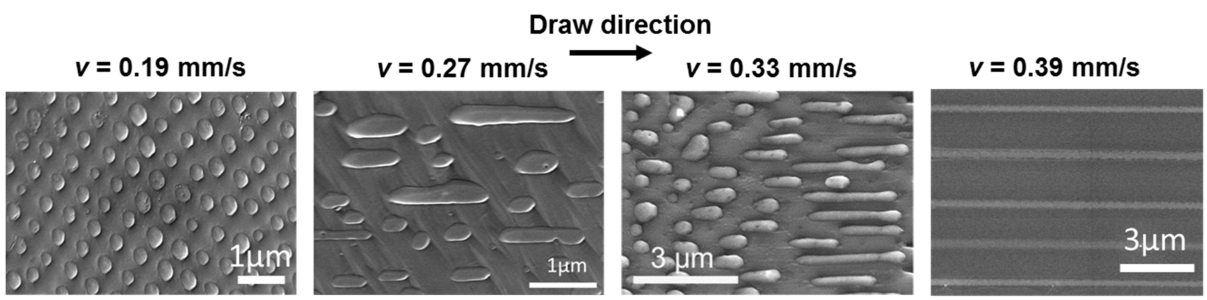


Figure S2: Plan view SEM images of bulk samples directionally solidified at different draw rates. Arrow indicates the draw direction.

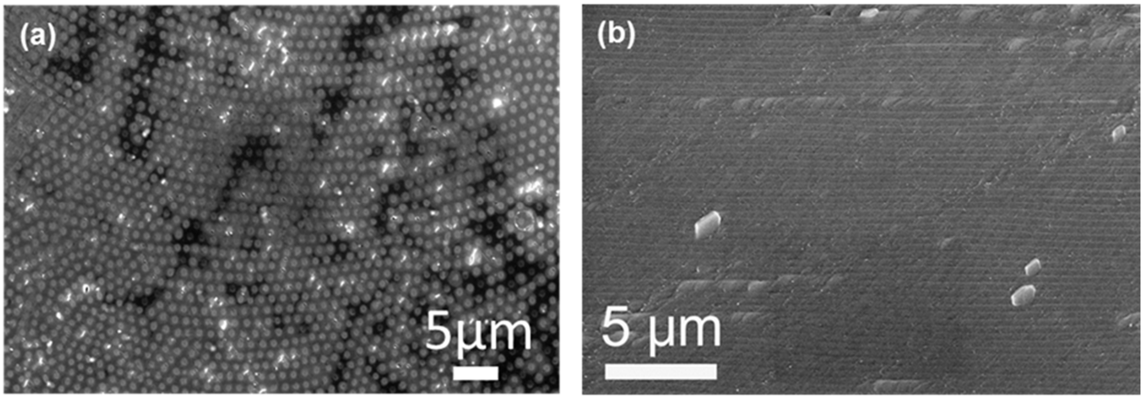


Figure S3: Low magnification plan view SEM images of bulk samples showing the (a) rod and (b) lamellar structure of the eutectic.

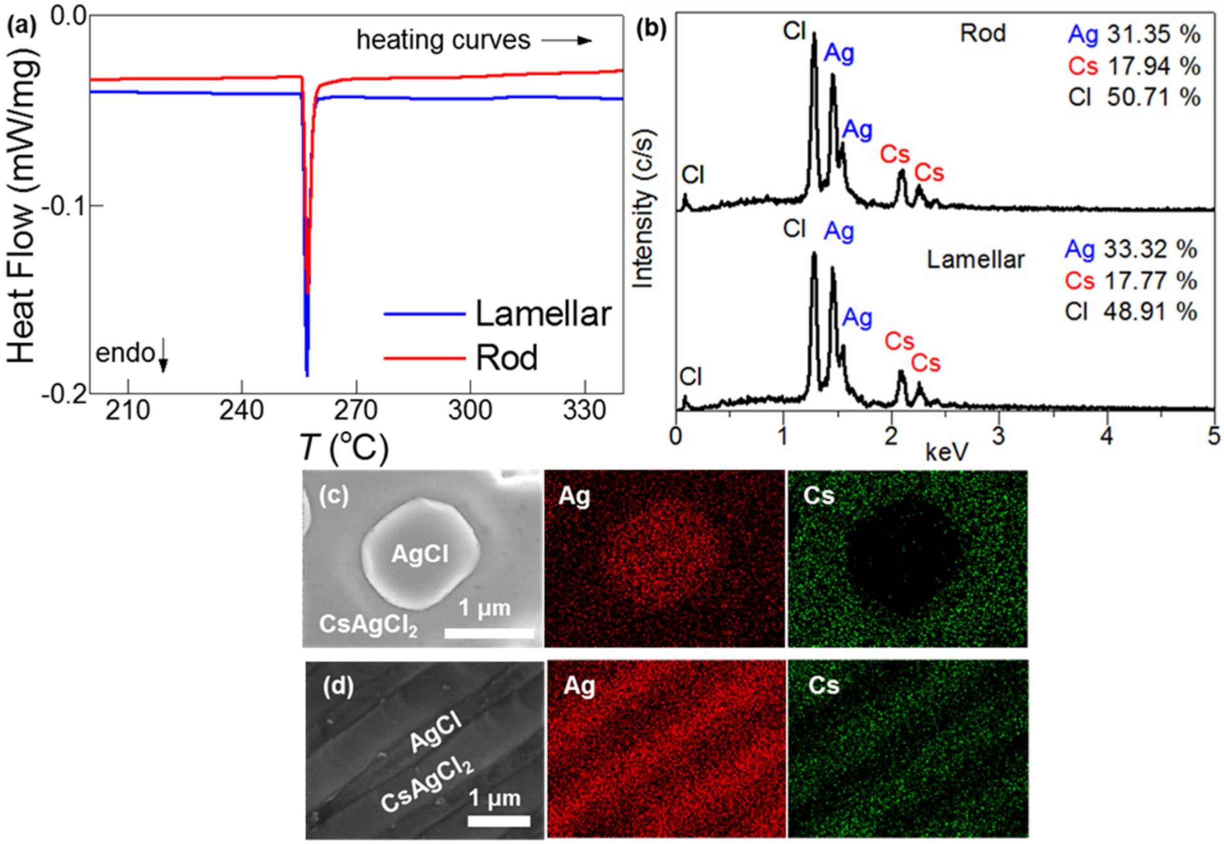


Figure S4: (a) Heat flow curves (taken with DSC) for samples with lamellar and rod structures, depicting the same melting points of 258 °C. (b) EDS analysis showing the at.% Ag, Cs and Cl as expected for the AgCl-$CsAgCl_2$ eutectic (Cs:Ag:Cl=1:2:3). Elemental mapping of Ag and Cs in the (c) rod and (d) lamellar microstructures of the eutectic.

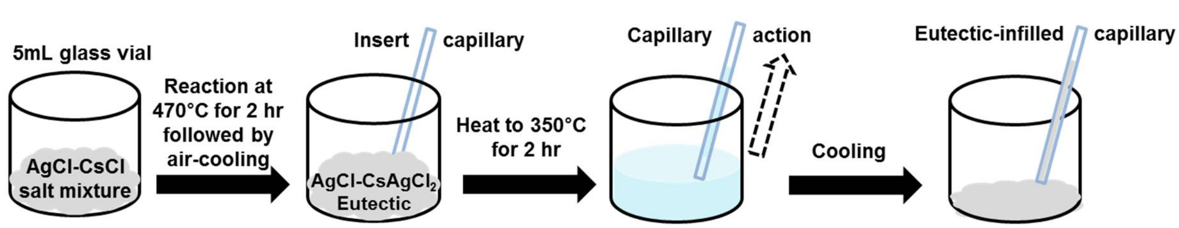

Figure S5: Schematic of the fabrication of a eutectic-infilled capillary.

Table S1: Parameters used in the phase field modeling, where α = $CsAgCl_2$ and β = AgCl phase.

| Parameter | Symbol | Units | Value | Reference |
|---|---|---|---|---|
| Eutectic Temperature | $T_E$ | K | 531 | (i) |
| Eutectic Composition | $C_E$ | mol % | 72 | (i) |
| α Phase Composition at $T_E$ | $C_\alpha$ | mol % | 50 | (i) |
| β Phase Composition at $T_E$ | $C_\beta$ | mol % | 100 | (i) |
| β Volume Fraction | $V_f$ | % | 36 | Calculated from (i) |
| α Liquidus Slope (at $T_E$) | $m_\alpha$ | K/mol% | -3.33 | Calculated from (i) |
| β Liquidus Slope (at $T_E$) | $m_\beta$ | K/mol% | 14.25 | Calculated from (i) |
| α Partition Coefficient (at $T_E$) | $k_\alpha$ | - | 0.694 | Calculated from (i) |
| β Partition Coefficient (at $T_E$) | $k_\beta$ | - | 1.389 | Calculated from (i) |
| α-Liquid Surface Tension (at $T_E$) | $\sigma_{\alpha L}$ | $mJ/m^2$ | 135 | Assumed $\sigma_{\alpha L} = \sigma_{\alpha\beta}$ |
| β-Liquid Surface Tension (at $T_E$) | $\sigma_{\beta L}$ | $mJ/m^2$ | 135 | Assumed $\sigma_{\beta L} = \sigma_{\alpha\beta}$ |
| α-β Surface Tension (at $T_E$) | $\sigma_{\alpha\beta}$ | $mJ/m^2$ | 135 | Extrapolated from (ii) |
| Eutectic Latent Heat of Fusion | $L_E$ | J/kg | $4.69 \times 10^4$ | Experiment (DSC) |
| α Latent Heat of Fusion | $L_\alpha$ | $J/m^3$ | $3.43 \times 10^8$ | Experiment (DSC) |
| β Latent Heat of Fusion | $L_\beta$ | $J/m^3$ | $5.13 \times 10^8$ | (iii) |
| Diffusion Coefficient (at $T_E$) | D | $m^2/s$ | $2.53 \times 10^{-10}$ | (iv) |
| α Contact Angle | $\theta_\alpha$ | ° | 30 | (v) |
| β Contact Angle | $\theta_\beta$ | ° | 30 | (v) |

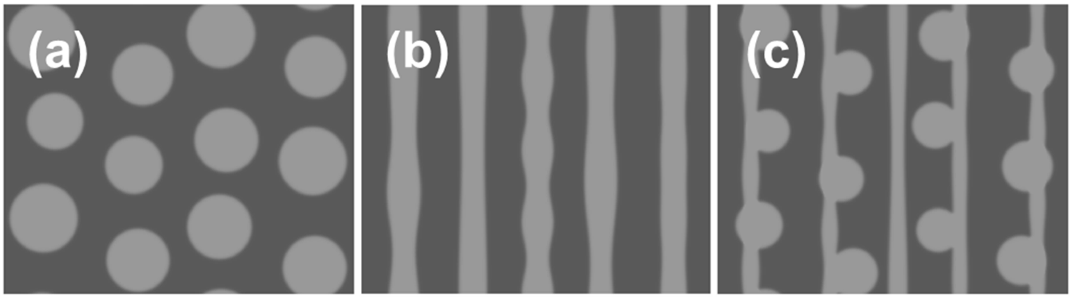


Figure S6: Cross-sections in the $y$-$z$ plane (perpendicular to the solidification direction) of the initial conditions (i.e. solid seed) for the eutectic structure as assumed during the phase-field simulations. Light gray and dark gray represent AgCl and $CsAgCl_2$, respectively. (a) Rod initial condition. (b) Lamellar initial condition. (c) Mixed rod and lamellar initial condition.

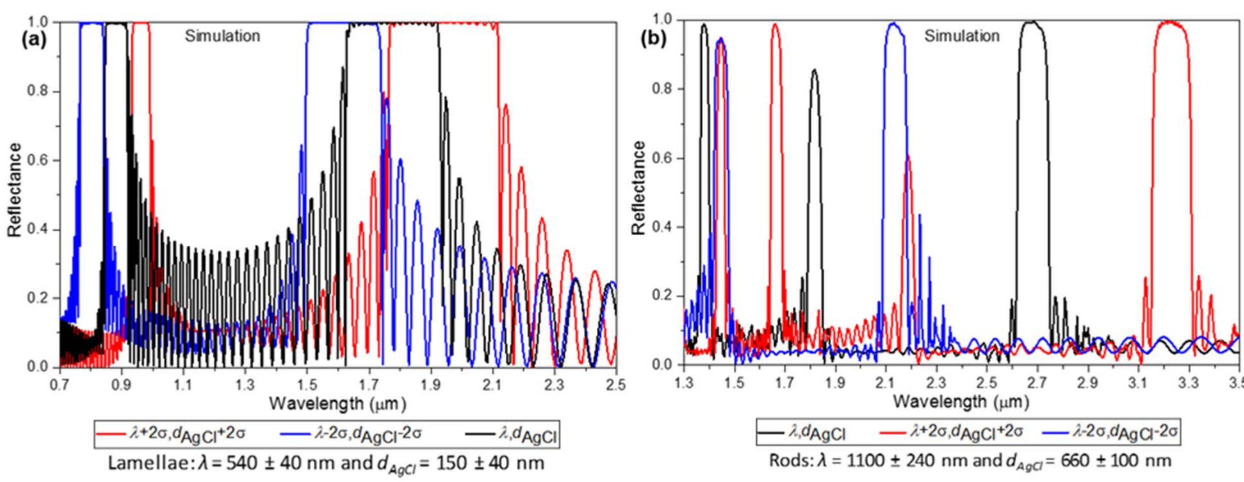

Figure S7: FDTD simulations showing the range of reflectance peaks for the experimentally observed size distribution in (a) lamellae and (b) rods.

References

(i) C. Sandonnini, G. Scarpa, *Rendiconti Accademia Lincei* **1912**, 21, 77.

(ii) S. Sternberg, M. Terzi, *Journal of Chemical Thermodynamics* **1971**, 3, 259.

(iii) W.T. Thompson, S.N. Flengas, *Canadian Journal of Chemistry* **1971**, 49, 1550.

(iv) S. Sternberg, C. Herdlicka, *Revue Roumaine de Chimie* **1972**, 17, 343.

(v) R. Folch, M. Plapp, *Physical Review E* **2005**, 72, 011602.